Science Advances
AAAS

advances.sciencemag.org/cgi/content/full/6/3/eaaw9727/DC1

Supplementary Materials for

When and how self-cleaning of superhydrophobic surfaces works

Florian Geyer, Maria D'Acunzi, Azadeh Sharifi-Aghili, Alexander Saal, Nan Gao, Anke Kaltbeitzel, Tim-Frederik Sloot, Rüdiger Berger, Hans-Jürgen Butt*, Doris Vollmer*

*Corresponding author. Email: butt@mpip-mainz.mpg.de (H.-J.B.); vollmerd@mpip-mainz.mpg.de (D.V.)

Published 17 January 2020, *Sci. Adv.* **6**, eaaw9727 (2020)
DOI: 10.1126/sciadv.aaw9727

The PDF file includes:

Other Supplementary Material for this manuscript includes the following:

(available at advances.sciencemag.org/cgi/content/full/6/3/eaaw9727/DC1)

Movie S1 (.mp4 format). Self-cleaning process of hydrophilic 10- to 50-μm particles.
Movie S2 (.mp4 format). Self-cleaning process of hydrophobic 10- to 50-μm particles.
Movie S3 (.mp4 format). Self-cleaning process of hydrophilic 1.5-μm particles.

Supplementary Materials and Methods

Synthesis of a fluorescent silica shell on 10–50 µm glass particles

The particles were coated according to the procedure described by D'Acunzi (*48*) and Verhaegh *et al*. (*49*). Glass beads (2 g; 10–50 µm) were washed and activated using the Fenton reagents (*50, 51*). The beads were dispersed in a solution prepared by slowly dissolving (*caution!*) iron sulfate heptahydrate (2 g) in 35 wt% hydrogen peroxide solution (20 mL). After 1 h, the particles were washed 3 times with water and 3 times with ethanol. Finally, they were dispersed in ethanol (80 mL), and reagents were added in this order: ammonia (6.4 mL), APS-RITC (0.17 mL; rhodamine B isothiocyanate coupled to (3-aminopropyl)triethoxysilane, see ref. (*48, 49*))), and tetraethoxysilane (TEOS, 0.480 mL). The mixture was kept under stirring for 24 hours and then washed 3 times with ethanol. The particle size was analyzed by scanning electron microscopy (SEM).

Synthesis of fluorescent silica particles

Fluorescent silica particles with diameters of 80 nm and 200 nm were synthesized by the same experimental procedure (see *Synthesis of a fluorescent silica shell on 10–50 µm glass particles*). The size was tuned by varying the amount of ammonia in the reaction mixture. Ethanol (160 mL) and ammonia (9.6 mL for 80 nm particles and 12.8 mL for 200 nm particles) were homogeneously mixed, and APS-RITC (0.34 mL) was added. After 1 min under stirring, TEOS (0.96 mL) was supplied. The mixture was kept under stirring for 24 h at 500 rpm. The particle suspension was washed 4 times with ethanol. The particle size was analyzed by SEM.

Synthesis of 1.5 µm polystyrene-silica core-shell particles with polystyrene core dyed with Nile Red

The polystyrene particles were prepared according to the procedure by D'Acunzi (*48*) and Zhang *et al.* (*52*). Polystyrene cores (PS) were synthesized by soap-free emulsion polymerization. Before starting the synthesis, the inhibitor was removed from the styrene by washing with 3 aliquots of 2 M sodium hydroxide solution and 3 aliquots of water. The washed styrene was distilled under reduced pressure before use. A 2000 mL three-necked flask was equipped with a condenser, a PTFE stirrer, and a gas inlet. Water (1000 mL) was put in the reactor and nitrogen was bubbled for 20 minutes. Ammonium persulfate (0.37 g) and sodium chloride (0.66 g) were dissolved in 10 mL water and put into the flask. After that, styrene (50 mL) and acrylic acid (0.66 mL) were added. The system was closed, and the mixture was heated to 75 °C under stirring at 350 rpm. After 1 day, the heating was turned off, and the mixture was cooled down to room temperature; particles were cleaned by at least 6 centrifugation steps with water and ethanol.

The polystyrene particles were dyed using the method described by Schaertl *et al.* (*53*). It is based on the preparation of a double-phase system formed by particles dispersed in water and Nile Red dissolved in xylene. Dye and xylene molecules diffuse through the water medium into the polystyrene particles. A solution of Nile Red (0.6 mg) in m-xylene (0.6 mL) was added to a dispersion of PS particles (1 g) in water (22 mL) and left under stirring for 1 day. After that time, the particles were swollen with xylene and dye. Xylene was removed by applying vacuum for 2 days. The particles were washed several times with water and ethanol and finally dispersed in ethanol (50 mL). A silica shell was grown on the

particles by adding ammonia (4.2 mL) and TEOS (1 mL) and leaving the system under stirring for 1 day. The particle size was analyzed by SEM.

Hydrophobization of the particles

The hydrophilic particles were dried and then suspended in 50 mL *n*-hexane. Afterwards, 50 µL of octyltrichlorosilane was added, the mixture was sonicated for 60 s and stirred at 250 rpm for 45 min. Then, the hydrophobized particles were washed with *n*-hexane for 3 times and dispersed in *n*-hexane.

Estimation of lateral adhesion force of a particle-covered substrate

This section describes the estimation of the force required to roll a drop over a layer of spherical particles of radius R on a superhydrophobic surface. The apparent contact area between the drop and the surface is supposed to have a width w. The density of particles on the substrate n (in number per unit area) is supposed to be lower than a full monolayer but large enough to support the drop and keep it from touching the substrate. We neglect forces between neighboring particles. When the drop moves a distance x in lateral direction, particles attached to the air-water interface are lifted because the apparent contact angles are high (Fig. 5). The work required to move the drop a distance x is

$$W = w \cdot x \cdot n \cdot W_\mathrm{s} \tag{1}$$

Here, W_s is the work required to detach a single particle from the substrate. The lateral force required to move the drop is

$$F_\mathrm{L} = \frac{\mathrm{d}W}{\mathrm{d}x} = w \cdot n \cdot W_\mathrm{s} \tag{2}$$

To obtain W_s we consider an individual particle in contact with the substrate and being attached to the air-water interface. When the drop moves, the particle at some point will find itself at the receding side. From the perspective of the particle, the air-water interface mainly moves upwards. It starts pulling on the particle. When pulling on a particle sticking at a liquid-air interface in the normal direction, the air-water interface deforms. The force increases linearly with the distance the particle is moved out of equilibrium (*54-57*).

The air-water interface acts as a spring with spring constant k (*40-42*)

$$k = \frac{2\pi\gamma}{0.8091 - \ln(R/l_\mathrm{C})} \tag{3}$$

Here, $l_C = \sqrt{\gamma/g\rho}$ is the capillary length. For water, it is 2.7 mm. Since the radius of curvature of the drop is much larger than the particle size, the interface can be described by a spring with spring constant k. With R = 25 µm, we get k = 0.082 N m^{-1}.

The capillary force pulls on the particle until the adhesion force between substrate and particle is overcome. The adhesion force F_{Adh} between a flat surface and a spherical particle is given, e.g., by the JKR theory (*43*)

$$F_{\mathrm{Adh}} = \frac{3}{2}\pi R\varphi(\gamma_{\mathrm{S}} + \gamma_{\mathrm{P}} - \gamma_{\mathrm{SP}}) \tag{4}$$

Here, γ_{S} is the surface energy of the substrate, γ_{P} is the surface energy of the particle and γ_{SP} is the interfacial energy between the two solids. Neglecting γ_{SP} and taking the surface energy of the fluorinated surface to be 10 mN m^{-1} and that of the hydrophilic oxide to be 100 mN m^{-1} we estimate $(\gamma_{\mathrm{S}} + \gamma_{\mathrm{P}} - \gamma_{\mathrm{SP}})$ =110 mN m^{-1}. Since the actual contact area is reduced on a superhydrophobic surface, we insert a factor φ. φ is the ratio of the actual to the apparent contact area of the particle. For the nanofilaments used in the experiment shown in Fig. 5, we estimate φ = 0.2 from SEM images. With R = 25 µm, we get 2.6 µN.

Capillary forces can usually overcome the adhesion forces. The capillary force can reach $F_{c,max} = 2\pi R\gamma\cos^2\frac{\theta}{2}$, where θ is the contact angle the particle forms with the air-water interface. If the actually applied force exceeds this value, the liquid will fully dewet the particle, and the capillary forces vanish. The air-water interface pulls on the particle until the particle detaches from the substrate. The deformation of the air-water interface at this point is $\delta = F_{\mathrm{Adh}}/k$. The work required to reach that point is

$$W_{\mathrm{s}} = \frac{1}{2}k\delta^2 = \frac{kF_{\mathrm{Adh}}^2}{2k^2} = \frac{F_{\mathrm{Adh}}^2}{2k} \tag{5}$$

To estimate n in our experiments, we assume that the large particles dominate. Their packing will not exceed the close random packing density of $0.82/(\pi R^2)$ (*58*). In our case, we estimate that the particle density is roughly a factor 2 lower. Thus, we take $n = 1/(10R^2)$. Putting everything together for an estimate and taking a typical width of $w \approx 0.5$ mm for 10 µL sized water drops, we obtain

$$F_L = wnW_{\mathrm{s}} = \frac{wF_{\mathrm{Adh}}^2}{20kR^2} = \frac{0.0005\mathrm{m}\cdot(2.6\times10^{-6}N)^2\mathrm{m}}{20\cdot0.082\mathrm{N}\cdot6.25\times10^{-10}\mathrm{m}^2} \approx 3\ \mu\mathrm{N} \tag{6}$$

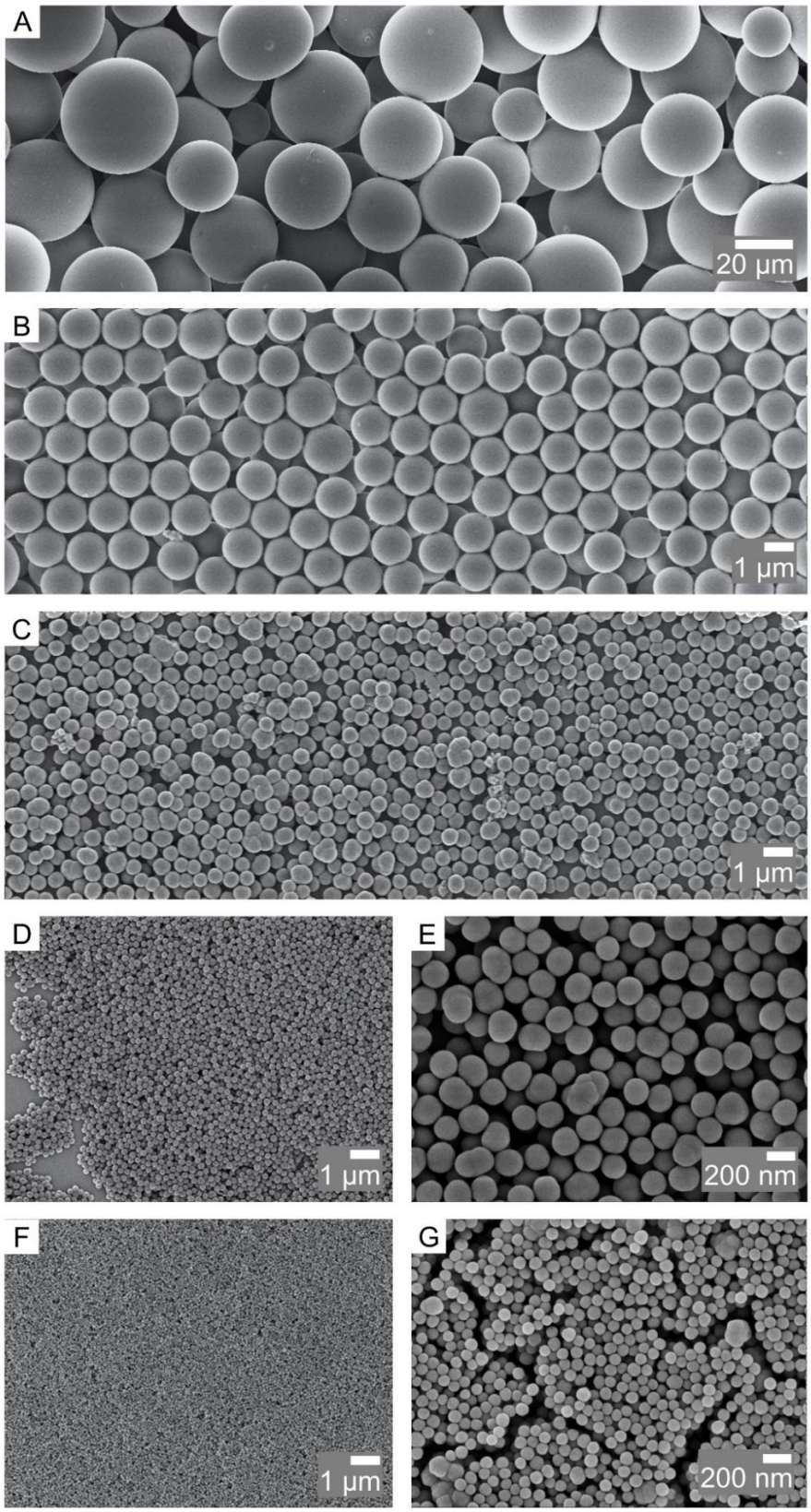

Fig. S1. SEM images of the model contamination particles. (**A** to **C**) SEM images of the hydrophilic 32±7 µm, 1.45±0.14 µm, and 580 ± 120 nm in diameter particles (denoted as 10–50 µm, 1.5 µm, and 600 nm particles) at different magnifications. (**D** and **E**) SEM images of the hydrophilic 210±30 nm (200 nm) particles. (**F** and **G**) SEM images of the hydrophilic 84±9 nm (80 nm) particles.

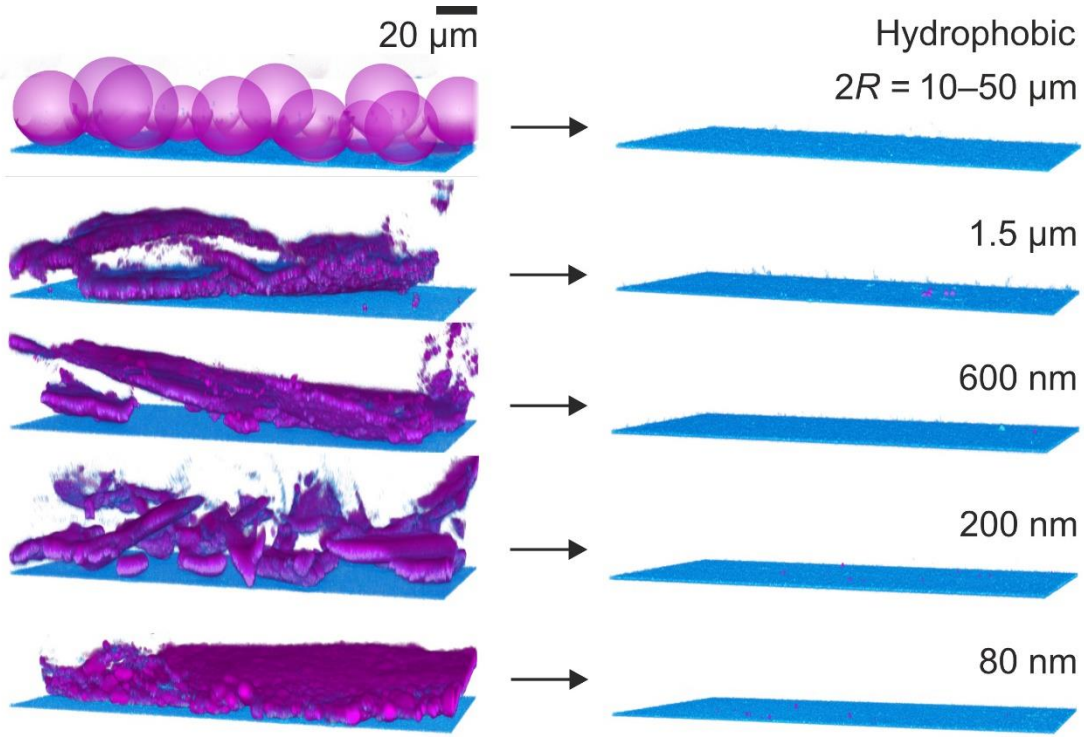

Fig. S2. LSCM images of nanoporous surfaces contaminated with hydrophobic particle powder. Representative LSCM images of the nanoporous surfaces (blue) contaminated with hydrophobic particle powder (purple) ranging between 80 nm and 50 µm before (left) and after self-cleaning (right). Some particle aggregates were not directly or easily cleaned, as the drops rolled over these hydrophobic aggregates but could eventually be removed.

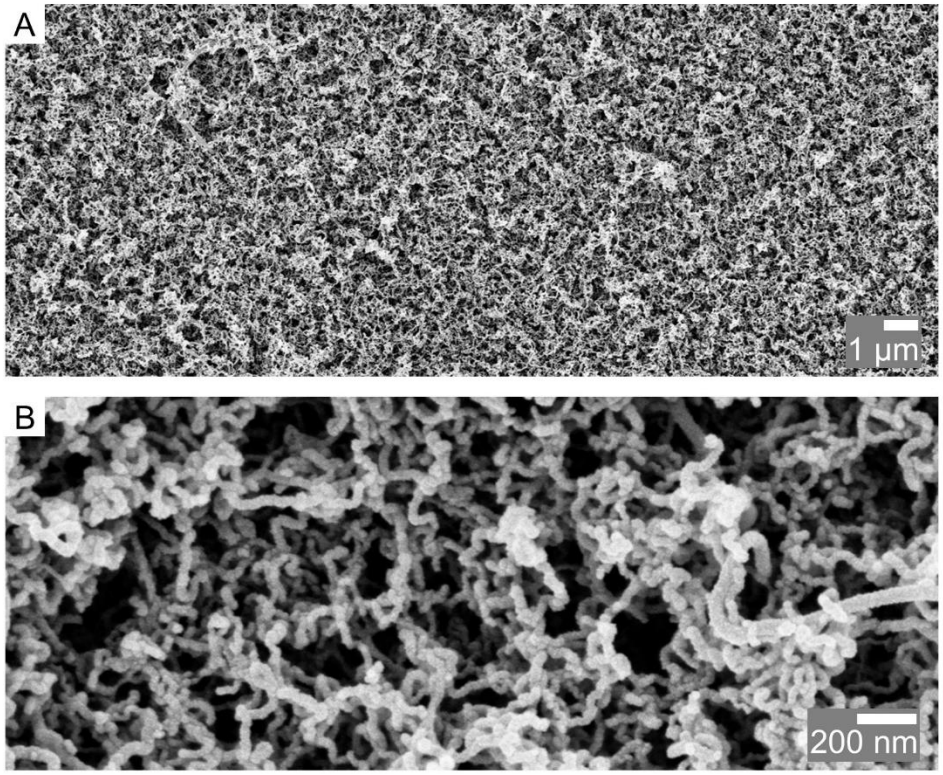

Fig. S3. SEM images of a nanoporous surface after contamination with hydrophobic 80-nm particles. (**A** and **B**) Representative SEM images at different magnifications of the nanoporous surfaces after contamination with 80 nm hydrophobic particle powder and subsequent self-cleaning.

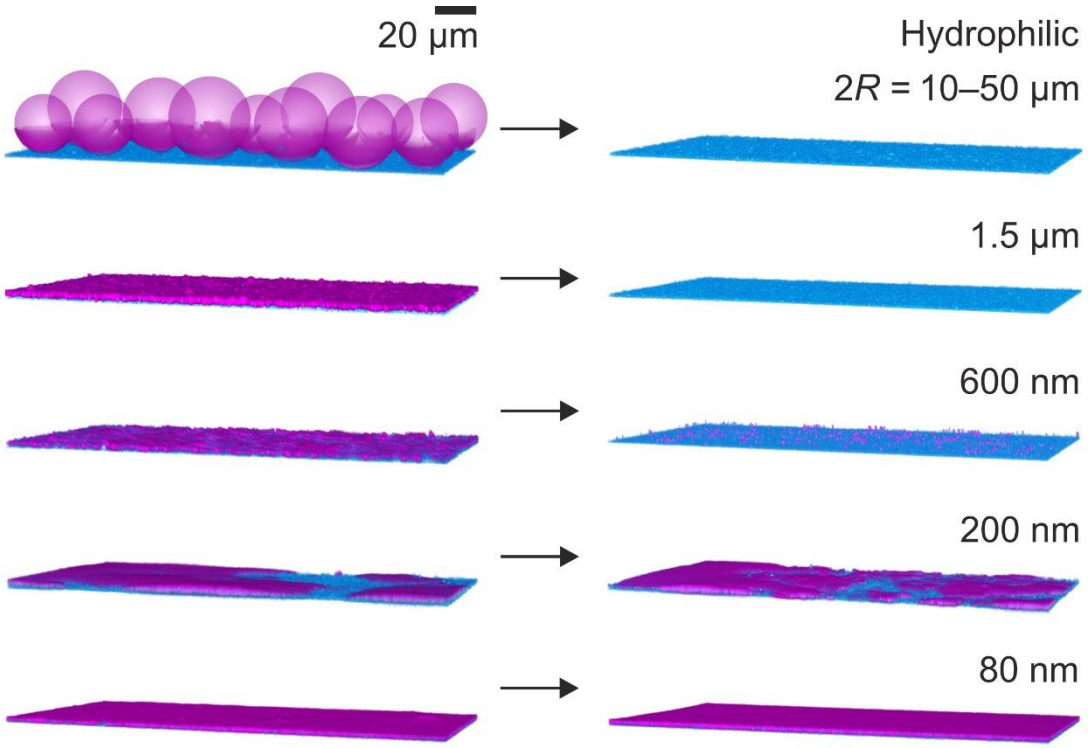

Fig. S4. LSCM images of nanoporous surfaces contaminated with hydrophilic particles from ethanol dispersion. Representative LSCM images of the nanoporous surfaces (blue) contaminated with hydrophilic particles (purple) ranging between 80 nm and 50 µm before (left) and after self-cleaning (right).

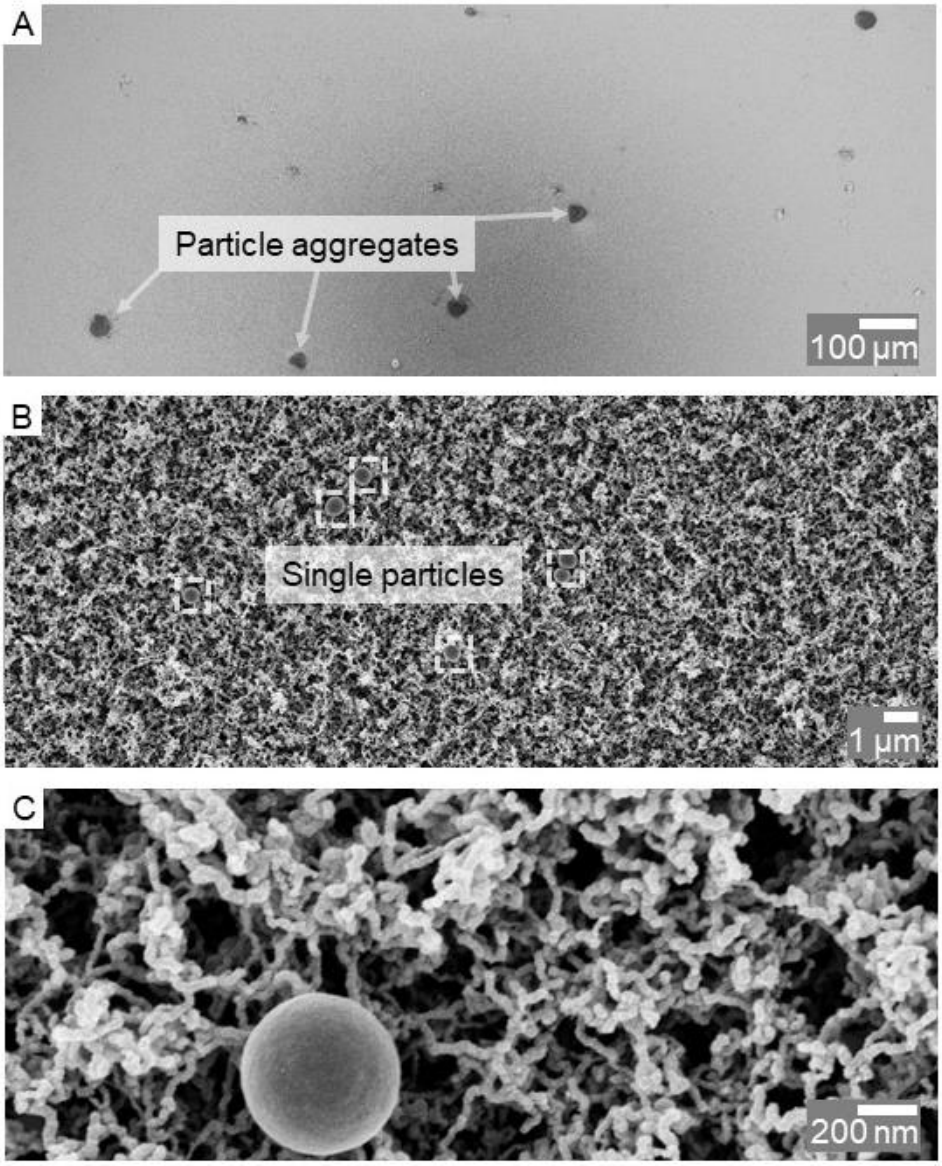

Fig. S5. SEM images of a nanoporous surface after contamination with a thin layer of hydrophilic 600-nm particles. (**A** to **C**) Representative SEM images at different magnifications of the nanoporous surface after contamination with 600 nm hydrophilic particles dispersed in ethanol and subsequent self-cleaning. Some particle aggregates cannot be easily removed by sliding water drops.

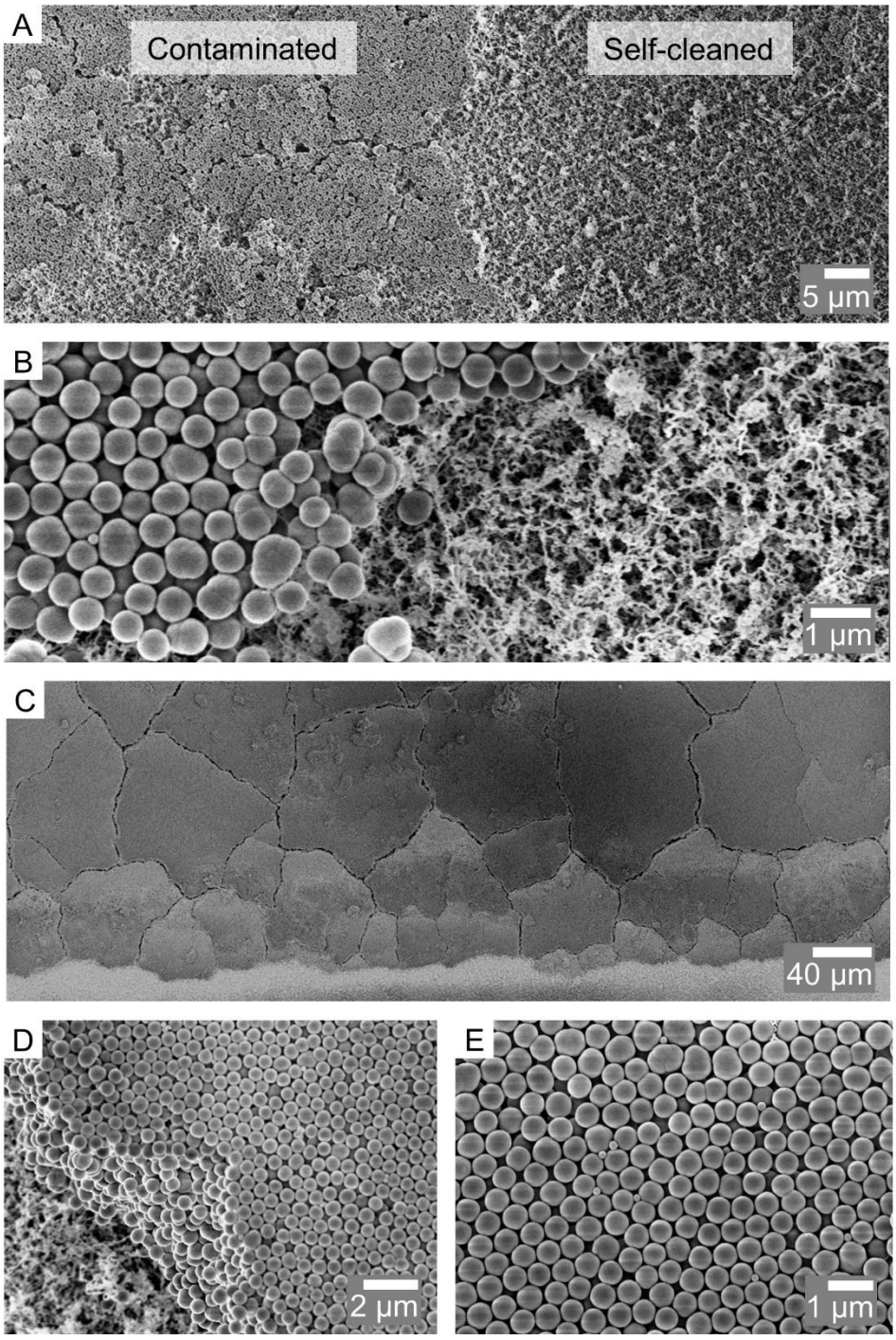

Fig. S6. Coffee stain effect during evaporation. (**A**) SEM image of a nanoporous superhydrophobic surface contaminated with hydrophilic 600 nm particles from ethanol dispersion. The image originates from a central region of the contaminated area. The left side shows the surface as is after contamination, the right side was self-cleaned using a few water droplets. (**B**) Higher magnification image of the transition zone between the contaminated and cleaned area. (**C**) SEM image of the outer side of the coffee stain ring. (**D**) Higher magnification image of the edge of the stain ring. (**E**) SEM image of the colloidal crystals formed at the coffee stain ring area.

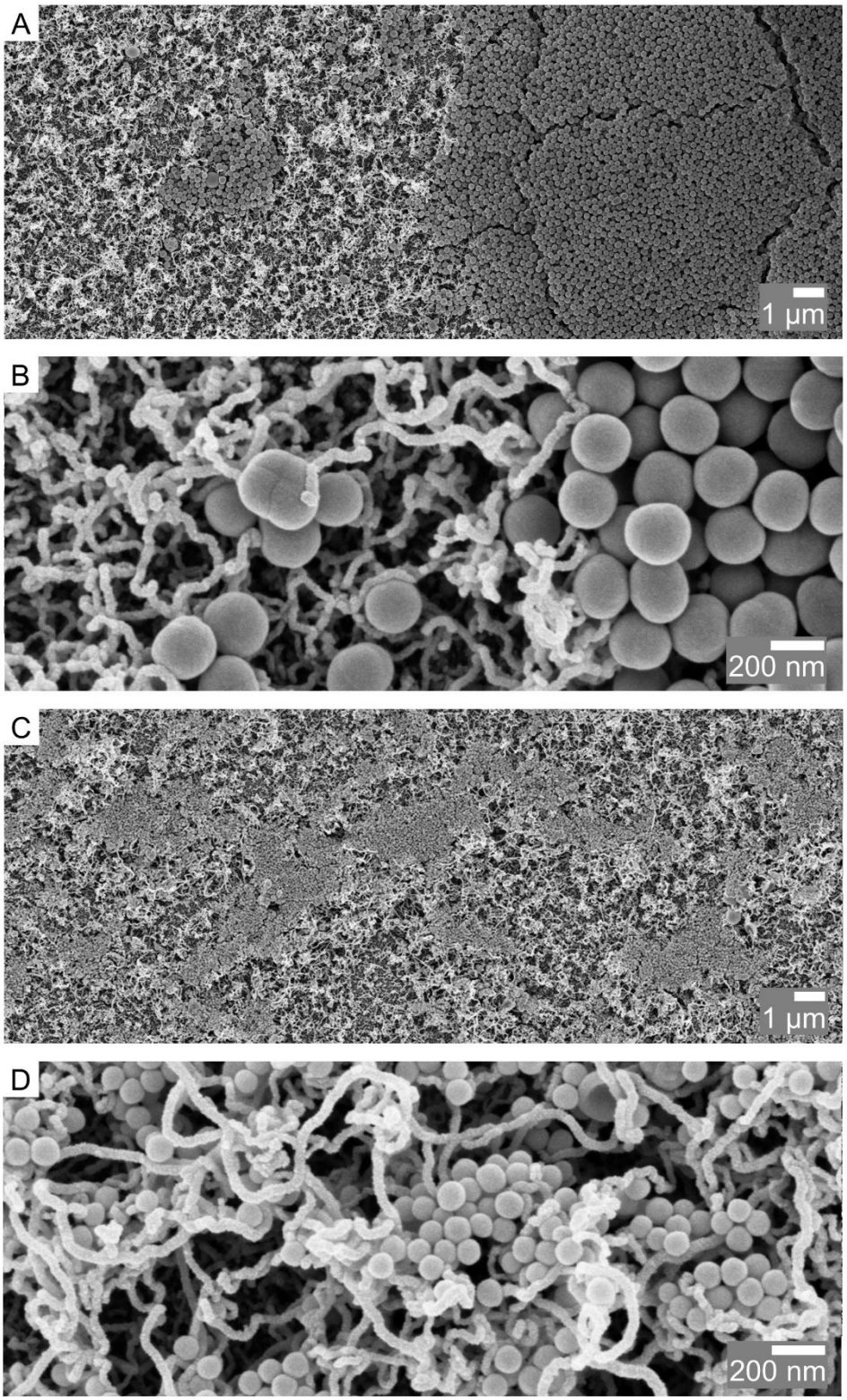

Fig. S7. SEM images of nanoporous surfaces after contamination with hydrophilic 200- and 80-nm particles. Representative SEM images at different magnifications of the nanoporous surfaces after contamination with 200 nm (**A** and **B**) and 80 nm (**C** and **D**) hydrophilic particles dispersed in ethanol and subsequent rinsing.

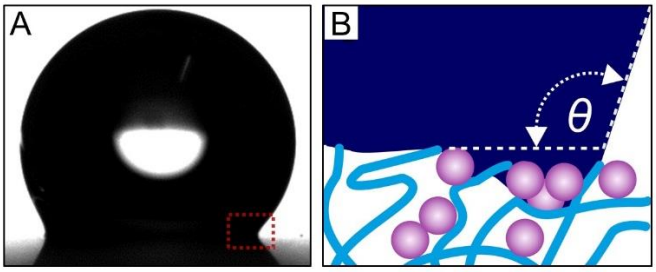

Fig. S8. Water droplet on a nanoporous surface contaminated with nanoparticles. (**A**) Optical photograph of a 6 µL droplet on a nanoporous superhydrophobic surface contaminated with hydrophilic 200 nm particles from ethanol dispersion. (**B**) Illustration of the contact line of a droplet on a contaminated surface where the spacing p between filaments is above the particle diameter, $p > 2R$. The droplet is in contact with the particles and the coating.

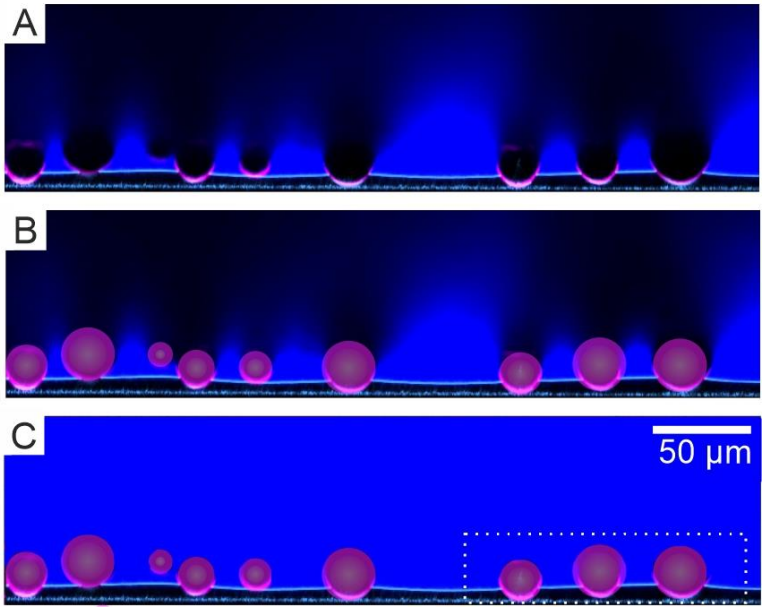

Fig. S9. Processing of the LSCM images. (**A**) Original image. Due to strong absorption and scattering of light, the upper part of the particle as well as the fluorescence of the aqueous solution above is not visible (black holes). (**B**) Particle illustrations are added based on the positions of the reflection and fluorescence at the lower side of the particles. (**C**) The missing fluorescence intensity above the particles, scale bars, and highlights are added to complement the image.

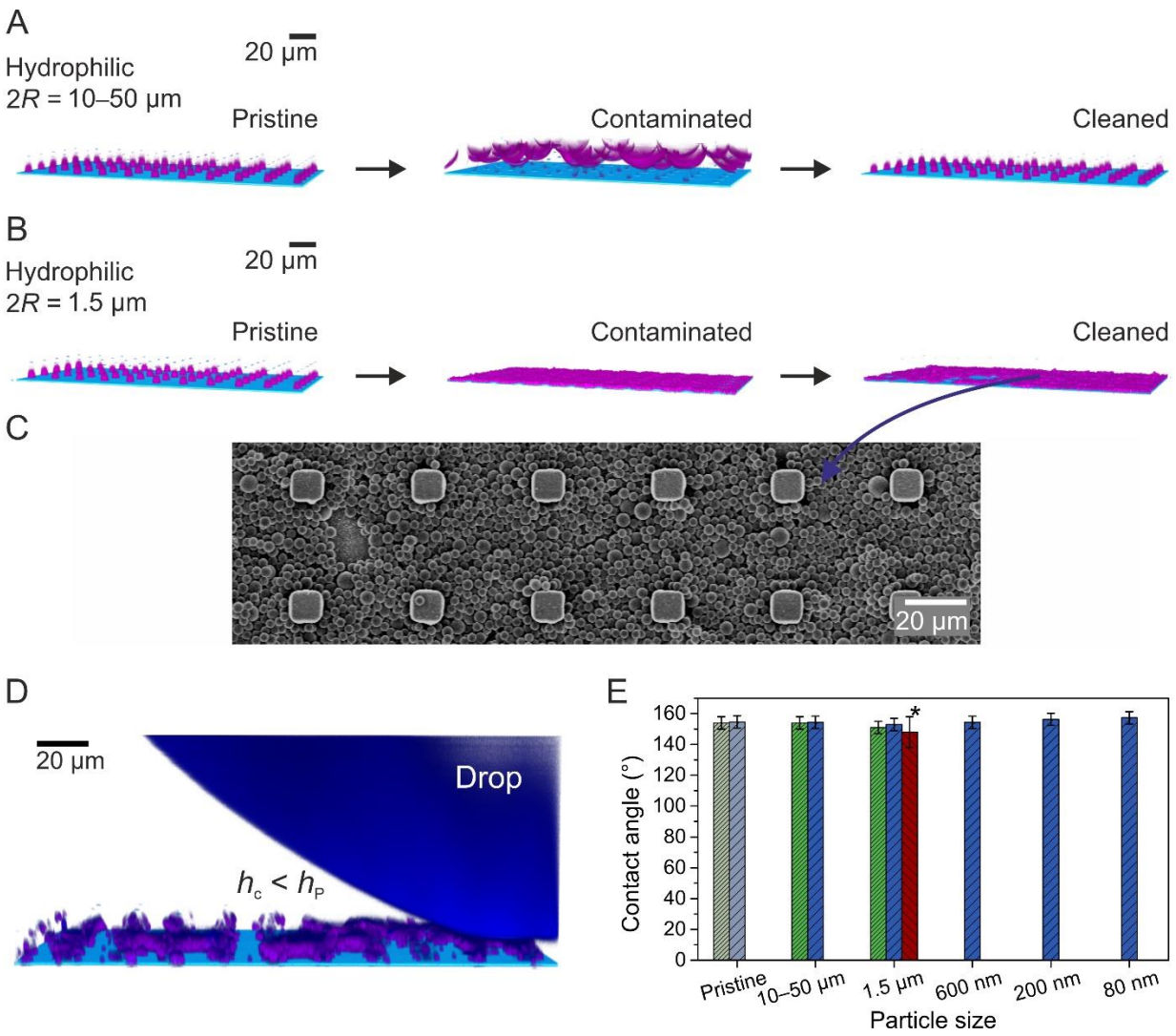

Fig. S10. Contamination and self-cleaning of superhydrophobic microstructured SU-8 pillars. For better visualization, the micropillars were fluorescently labeled. **(A)** Microstructured surface after contamination and self-cleaning with 10–50 µm hydrophilic particles. The large particles cannot enter the structure and thus can be easily cleaned. (**B**) Microstructured surface after contamination and self-cleaning with hydrophilic 1.5 µm particles from ethanol dispersion. The particles can enter the structure and remain there even after self-cleaning. The surface still remains intact. (**C**) SEM image showing the 1.5 µm particles between the micropillars. The particles do not completely fill up the array. Particles on the top faces of the pillars were removed. **(D**) LSCM image showing a 10 µL water drop (dyed with ATTO488) on a micropillar surface contaminated with hydrophilic 1.5 µm particles where $h_c < h_P$. The drop rests on the top face of the micropillars. (E) Static contact angles using 6 µL water drops after contamination of the micropillar array with hydrophilic and hydrophobic particles of various sizes and subsequent self-cleaning. *For $h_c \geq h_P$, it is important to note that the contact angle corresponds to the surface after cleaning. On a SU-8 micropillar surface which is completely covered with particles ($h_c >> h_P$) and before cleaning, the droplet spreads on the surface (contact angle $\theta \approx 0$). However, the deposition of droplets leads to a cleaning, but not self-cleaning, effect. The particles are slowly dissolved in the aqueous phase, and eventually the surface is partially cleaned, leaving particles left at the walls of the fluorinated pillars. Pinning at the contaminated pillars causes the high static contact angle.

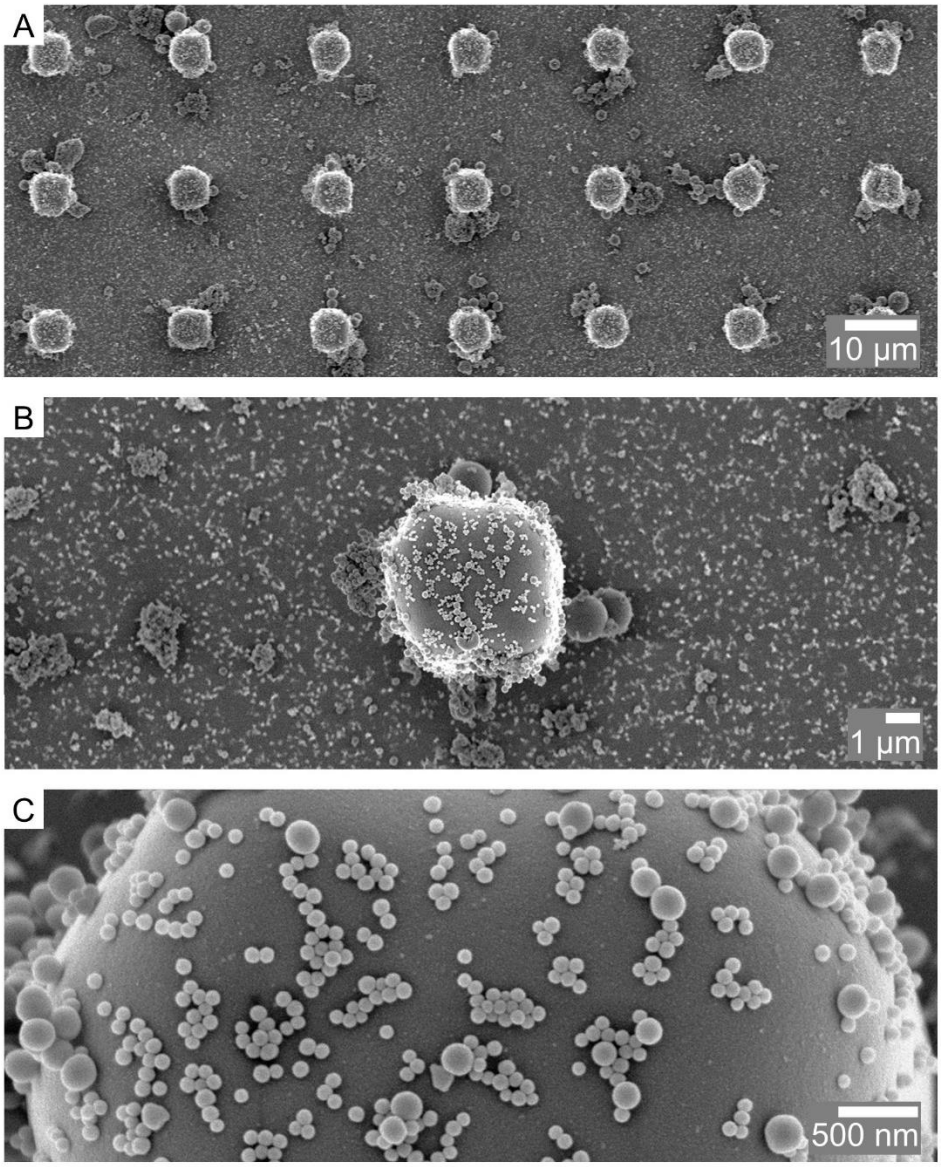

Fig. S11. SEM images of superhydrophobic microstructured SU-8 pillars after contamination with hydrophobic particles. (**A** to **C**) SEM images of the superhydrophobic microstructured SU-8 pillar surface which was consecutively contaminated with powders of the hydrophobic particles (50 µm to 80 nm). After self-cleaning, 600 nm and especially 200 nm as well as 80 nm particles remained on the surface, providing an additional roughness and resulting in lower roll-off angles.

Fig. S12. Photographs of the superomniphobic fabrics on the car after 257 days of outdoor exposure. (**A**) Superomniphobic fabrics fixed on the front window. (**B**) Fabric fixed on the left mirror. (**C**) Fabric fixed on the rear side window. (**D**) Fabrics fixed on the rear window. All superomniphobic fabrics remained white without any obvious stains.

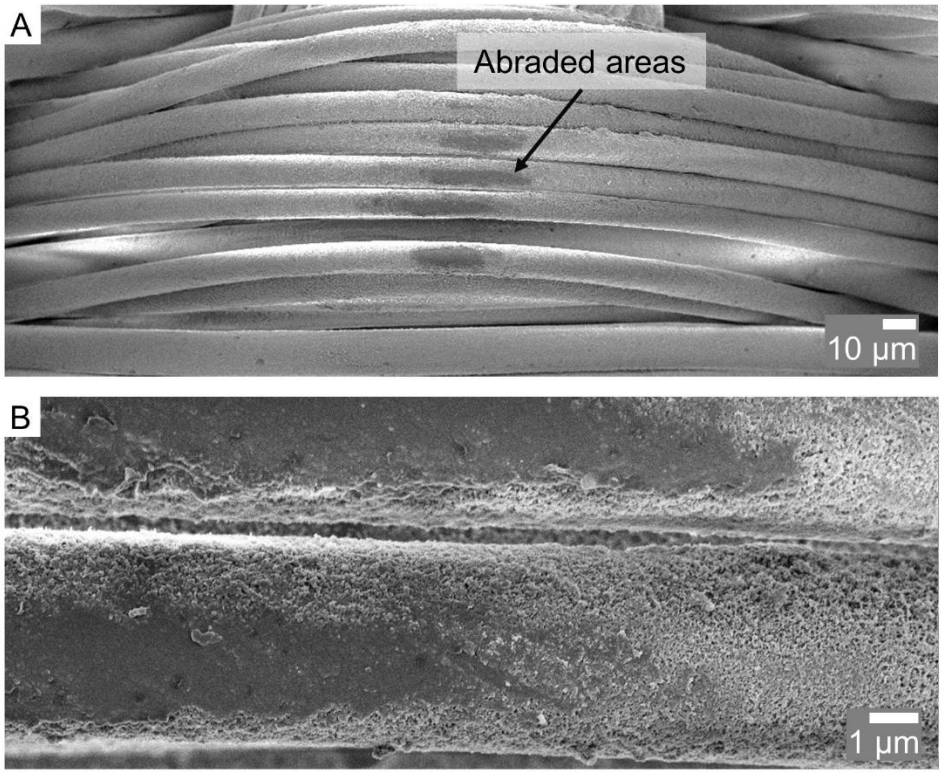

Fig. S13. SEM images of abraded microfibers. SEM images of the fabric which was fixed at the mirror after an outdoor exposure of 257 days. (**A** and **B**) Different magnifications of the fabric showing some abraded top faces of the nanofilament-coated polyester microfibers.

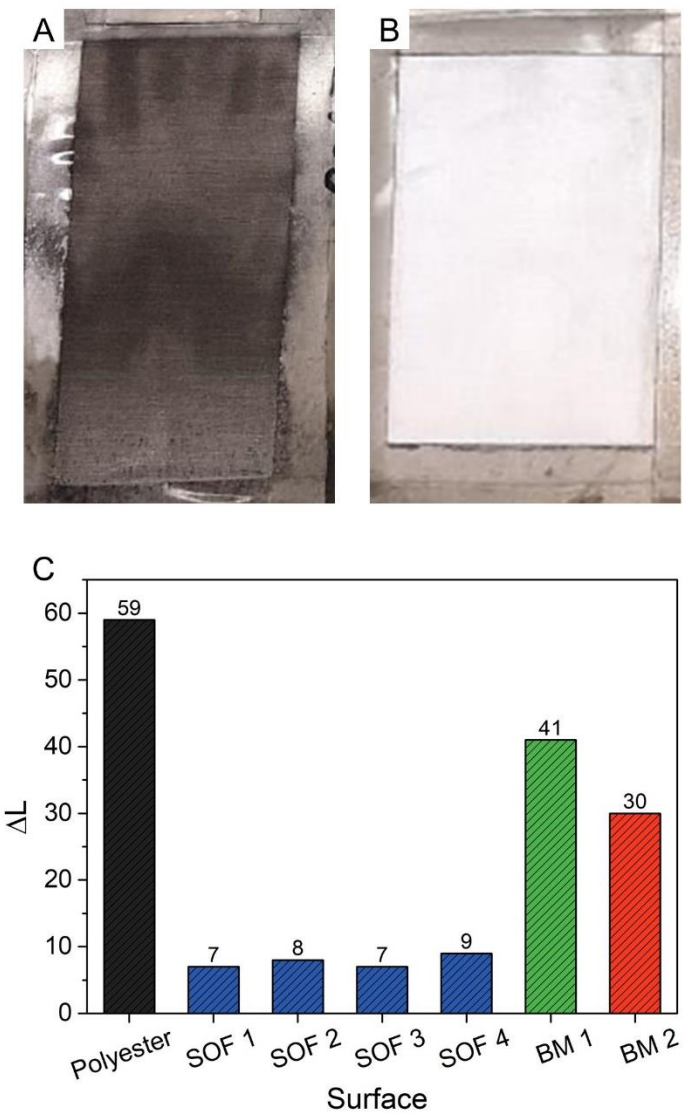

Fig. S14. Industrial contamination test. Photographs of a bare (**A**) and superomniphobic fabric (**B**) after the industrial standardized contamination resistance test, conducted by Evonik Resource Efficiency GmbH. The bare fabric turned black due to pickup of contamination whereas the superomniphobic remained white. (**C**) Industrial standardized contamination resistance test for easy-to-clean surfaces, conducted by Evonik Resource Efficiency GmbH. The tested surfaces included a bare polyester fabric, superomniphobic fabrics (SOF) and two benchmark surfaces (BM).

Table S1. Temperatures (*T*) and rainfall and humidities (RH) during the outdoor exposure of the superomniphobic fabrics. Temperatures and rain total were collected from www.wetterkontor.com. The humidities from www.timeanddate.de.

Period [days]	Min. T [°C]	Max. T [°C]	Avg. min. T [°C]	Avg. max. T [°C]	Avg. T [°C]	Rain total [L/m^{-2}]	Avg. min. RH [%]	Avg. max. RH [%]
0–4	5.1	13.6	6.7	12.4	9.1	0.8	54	76
22–56	-5.4	15.3	3.0	8.4	5.7	40.6	69	93
92–133	-9.6	10.6	-1.9	3.3	0.6	32.5	66	90
189–249	-0.9	32.0	9.0	18.9	13.9	94.6	46	87
308–426	-2.8	29.1	8.3	15.5	11.8	194.7	65	96

Movie S1. Self-cleaning process of hydrophilic 10- to 50-µm particles on a nanoporous superhydrophobic surface using a 10 µL water drop (dyed with ATTO488) recorded by the LSCM. After the initial self-cleaning, the drop is rolled back.

Movie S2. Self-cleaning process of hydrophobic 10- to 50-µm particles on a nanoporous superhydrophobic surface using a 10 µL water drop (dyed with ATTO488) recorded by the LSCM. After the initial self-cleaning, the drop is rolled back.

Movie S3. Self-cleaning process of hydrophilic 1.5-µm particles on a nanoporous superhydrophobic surface using a 10 µL water drop (dyed with ATTO488) recorded by the LSCM. After the initial self-cleaning, the drop is rolled back.

Note S1. Imaging self-cleaning.

To demonstrate self-cleaning, drops are commonly imaged from the side or top using optical photography or video microscopy while rolling over contamined surfaces (*59*). Because of the high contact angle and the high depth of field, optical photography or video microscopy cannot provide detailed insight of the region close to the three-phase contact line (fig. Note S1). It is hardly possible to determine the precise position of the three-phase contact line for superhydrophobic surface showing contact angles above 150° using video microscopy (*26*). This problem becomes even worse in the presence of contamination (fig. Note S1B). Photographs taken from the top do not provide any information about the contact line (fig. Note S1, C to F). This limitation can be overcome using laser scanning confocal microscopy (see Fig. 4).

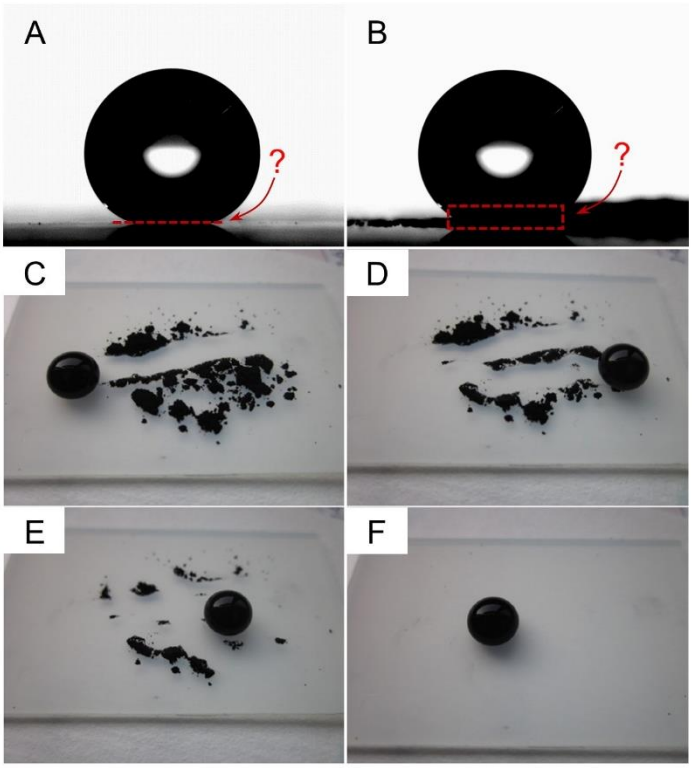

Fig. Note S1. Imaging self-cleaning using commonly employed methods. (**A**) Droplet (6 µL) on a superhydrophobic surface. The precise determination of the three-phase contact line is difficult for high contact angles (> 150°). (**B**) Droplet (6 µL) on a contaminated superhydrophobic surface. The shape of the three-phase contact line cannot be determined because it is obscured by the contamination particles due to the depth of field. (**C** to **F**) Self-cleaning of graphite powder (black) on a superhydrophobic surface. Reproduced from ref. (*59*). Copyright 2013, Elsevier.